XANES Evidence Against a Manganyl Species in the S_3 State of the Oxygen-Evolving Complex

Tsu-Chien Weng, Wen-Yuan Hsieh, Erich S. Uffelman, Scott W. Gordon-Wylie, Terrence J. Collins, Vincent L. Pecoraro,* and James E. Penner-Hahn*

Department of Chemistry and the Biophysics Research Division, The University of Michigan, Ann Arbor, Michigan 48109-1055, and the Department of Chemistry, Carnegie-Mellon University, Pittsburgh, Pennsylvania 15213

Received February 2, 2004; E-mail: vlpec@umich.edu; jeph@umich.edu

The oxygen-evolving complex (OEC) of photosystem II (PS II) is responsible for the four-electron conversion of water to dioxygen via photooxidation of a tetranuclear manganese cluster.[1-3] Four photon-induced charge separations drive transitions between five oxidation levels named S_0-S_4. The most oxidized species, S_4, is unstable, releasing O_2 and regenerating S_0. On the basis of XAS and EPR data, it is generally accepted that S_1, the dark-stable oxidation level, contains a $Mn^{III}_2Mn^{IV}_2$ cluster and that production of S_2 results in a metal-centered oxidation to $Mn^{III}Mn^{IV}_3$.[4-6] For S_3, there are conflicting claims: oxidation of Mn[7] would give Mn^{IV}_4, while ligand-centered oxidation[6] would give a radical on either protein or substrate.

Recently, the manganyl moiety, either $Mn^{IV}=O$ (formal bond-order 2.5) or $Mn^V\equiv O$, has been suggested to be catalytically important in one or more of the higher S-states. Babcock and co-workers suggested (Scheme 1) that $Mn^{IV}=O$ is formed in S_3 and is a precursor for the active water oxidant in S_4.[8] We and others have suggested that either $Mn^{IV}=O$(radical) or $Mn^V\equiv O$ may be formed in S_4,[9,10] and a synthetic complex has been suggested to use $Mn^V\equiv O$ in water oxidation.[11] Manganyl is electrophilic and could be attacked by a nucleophilic water or hydroxide, bound either to manganese or calcium, to form an O–O bond. In addition to this potential biological relevance, manganyl $Mn^V\equiv O$ complexes have also garnered considerable attention as the proposed reactive species in asymmetric olefin epoxidation.[12-14]

Although a few mononuclear $Mn^V\equiv O$ complexes have been crystallographically characterized,[15-17] X-ray absorption spectroscopy (XAS) of $Mn^V\equiv O$ complexes has not been reported. XAS data for Ti, V,[18] and Cr[19] metal–oxo species all show an extremely intense preedge feature that is polarized along the M–O axis. The energy of the preedge transition corresponds to a 1s → 3d transition, but the intensity is significantly higher than is normally seen. The unusually high intensity of the $M\equiv O$ preedge features indicates significant p-symmetry in the final state, presumably as a consequence of M(3d) + O(2p) orbital mixing.[19] Ferryl complexes have a much weaker preedge feature.[20-24] This was attributed to the fact that for Fe^{IV}, the Fe–O antibonding orbitals are occupied, thus lengthening the Fe–O bond and decreasing the M(3d) + O(2p) overlap.[19] In this study, we report XAS data for $Na[Mn^V\equiv O(HMPAB)]$, **1**, a crystallographically characterized species containing the manganyl unit.

Complexes **1** and **2** ($Na[Mn^{III}(HMPAB)(EtOH)_2]$) were prepared as previously described.[15] XAS data were measured for solid **1** at NSLS and for solutions of **1** (acetonitrile) and **2** (ethanol) at APS.[25] Near-edge spectra (Figure 1) show a weak preedge transition for **2** but a strong preedge transition for **1**. The latter reaches nearly one-third of the edge jump and is thus very similar to the preedge feature seen for the iso-electronic $Cr^{IV}=O$. In addition to the change in preedge intensity, there is a shift of the edge to higher energy on

Scheme 1 [a]
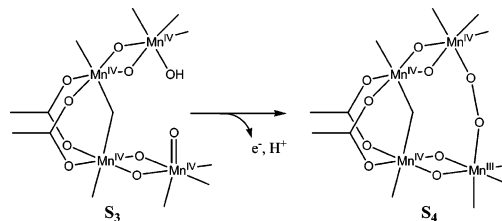
[a] Redrawn from ref 8.
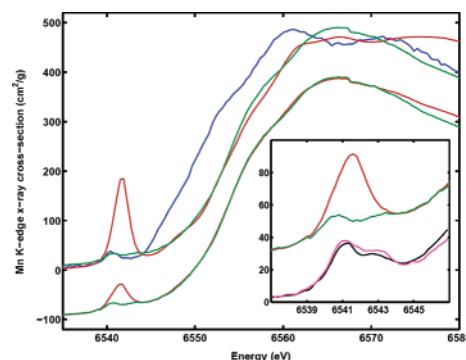
Figure 1. (Top) XANES spectra for **1** (red), **2** (blue), and **3** (green). (Bottom) Simulated XANES for hypothetical $Mn^{IV}_3Mn^V=O$ (red) and authentic Mn^{IV} (**3**, green) structures. For comparison, XANES spectra[6] for pure S_2 (black) and S_3 (pink) states of the OEC are also shown (inset).

going from Mn^{III} to Mn^V. The solid-state spectrum for **1** (not shown) is identical to that in solution. The edge energy for $[Mn^{IV}_2(2\text{-OH-}3,5\text{-di-}(t\text{-Bu-salpn})](NO_3)_2$, **3**, is nearly identical to that for **1**.

Although detailed interpretation of edge structure is difficult, there is significant empirical data correlating edge energy with metal oxidation state. Using the first moment to determine the energy for a library of Mn model compounds, we find that the edge energy increases by ~4 eV for every unit increase in formal oxidation state on going from Mn^{II} to Mn^{III} to Mn^{IV} (Table S1). However, the edge energies for **1** and **3** are virtually identical (Figure 1). Consequently, while oxidation of Mn^{III} to Mn^{IV} is readily detectable, even when only 1 of 4 Mn is oxidized,[26] the data in Figure 1 suggest that edge energy may not give a reliable indication of whether Mn has been oxidized from Mn^{IV} to $Mn^V\equiv O$.

The EXAFS spectra for **1** and **2** (Figure 2) both show a main peak at $R + \alpha \approx 1.5$ Å and a poorly resolved outer-shell peak at 2.2 Å that can be assigned as Mn–(N/O) and next-nearest-neighbor Mn–C, respectively. Peaks are shifted by ca. 0.4 Å to lower R relative to the true M–L distance.[25] More distant HMPAB atoms do not make a significant contribution, presumably due to disorder. The FT amplitude for **1** is lower than that for **2**, but does not show a resolved peak attributable to the short $Mn\equiv O$. EXAFS curve
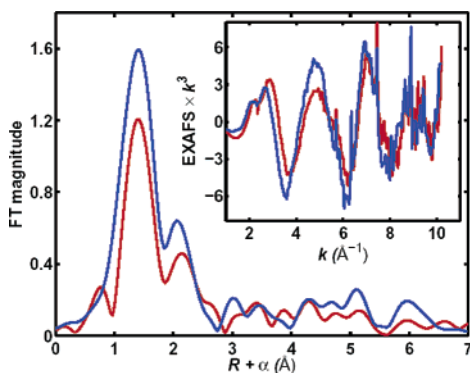
Figure 2. k^3-weighted EXAFS data (inset) and Fourier transforms of the EXAFS for **1** (red) and **2** (blue).

fitting (see Table S1) gave results consistent with the crystal structures of **1** and **2**. In particular, **1** could not be fit without including a short Mn−O distance, despite the absence of a resolved Mn≡O peak in the FT.

EXAFS data for the OEC is usually limited to $k_{max} \approx 11.5$ Å^{-1} by the presence of iron. In contrast, the EXAFS data for solid **1** extends to 14.4 Å^{-1}, allowing us to study the effect of k range on the ability to resolve short Mn≡O distances. Three-shell fits (Mn≡O, Mn−(N/O), Mn−C) are always better than two-shell fits, regardless of k range (see Table S1). However, the apparent Mn−O distance varies from 1.55 to 1.72 Å depending on the k range. We attribute this to the fact that the Mn≡O and Mn−(N/O) EXAFS signals are approximately out of phase, so that a small change in the spline background can alter significantly the apparent frequency of the low-frequency Mn≡O oscillations. It is noteworthy that the Mn≡O oscillations contribute to the low-R region ($R \leq 1.0$ Å) region; if the structure were unknown, Fourier filtering could inadvertently alter the Mn≡O signal.

Although we obtain reasonably accurate Mn≡O distances when fitting the data for **1**, it would be difficult to identify unambiguously the presence of a short Mn≡O bond using EXAFS alone. It becomes nearly impossible to identify one short Mn−O bond distance (1.55 Å) from the other 22 Mn−(N/O) bonds between 1.8 to 1.9 Å when fitting synthetic EXAFS data designed to mimic a putative Mn$^{IV}_3$Mn^V state (i.e., 75% **3** + 25% **1**) over a short k range (1.0−11.5 Å^{-1}).

In contrast to the insensitivity of EXAFS and edge energy to Mn≡O, it should be possible to use the preedge *intensity* to identify the presence of Mn^V≡O in the OEC. Preedge spectra for crystallographically characterized Mn compounds of various oxidation states were fit using a pseudo-Voigt function (see Table S2). The preedge peak energy increases only slightly (ca. 1 eV) on going from Mn^{II} to Mn^V, and the preedge area does not depend strongly on oxidation state. Most of the complexes have a preedge area between 15 and 75 cm^2·eV/g, with the exception of oxo-bridged Mn^{IV} complexes that have areas of up to 150 cm^2·eV/g. Complex **1** has an area of 551 cm^2·eV/g (vs 1013 for KMnO$_4$ and 60 cm^2·eV/g for complex **2**). The preedge area predicted for Mn$^{IV}_3$Mn^V≡O complex is ∼8-fold larger than that of Mn^{IV}−(μ-alkoxy)$_2$−Mn^{IV} (Figure 1). Even if only 12% of Mn$^{IV}_3$Mn^V≡O was formed, we would still observe a near doubling in preedge area. Therefore, the absence of an increase in preedge intensity in published S$_3$ spectra[6,7] (inset to Figure 1) is evidence *against* the formation of Mn^V≡O in S$_3$.

In the absence of an authentic model, it is difficult to know exactly what the XANES for Mn^{IV}≡O would look like, since this could have a longer Mn−O bond and thus a weaker preedge transition. For Fe, the increase in 1s → 3d intensity on forming a

d^4 Fe^{IV}≡O complex[20−23] is 6 times smaller than the increase on forming the d^2 Cr^{IV}≡O[19] or Mn^V≡O.[25] If the increase on forming a d^3 Mn^{IV}≡O is the average of these, the preedge would still be sufficient to exclude the presence of 25% Mn$^{IV}_3$Mv^{IV}≡O in S$_3$.

These observations allow us to assess previous models for water oxidation. The H-atom abstraction mechanism that has had recent popularity (Scheme 1) invokes an Mn≡O moiety in S$_3$. Our present analysis shows that the preedge transition is the most reliable method for investigating the presence of Mn≡O species and further suggests such a structure is *not* found in the OEC before the production of S$_4$. It may, therefore, be appropriate to reconsider the validity of mechanisms that invoke Mn≡O prior to the catalytically active S$_4$ state.

Supporting Information Available: Tables of fitting results for EXAFS and XANES; description of data collection and analysis procedures. This material is available free of charge via the Internet at http://pubs.acs.org.

References

(1) Debus, R. J. *Biochim. Biophys. Acta* **1992**, *1102*, 269−352.
(2) Yachandra, V. K.; Sauer, K.; Klein, M. P. *Chem. Rev.* **1996**, *96*, 2927−2950.
(3) Tommos, C.; Babcock, G. T. *Acc. Chem. Res.* **1998**, *31*, 18−25.
(4) Yamauchi, T.; Mino, H.; Matsukawa, T.; Kawamori, A.; Ono, T. *Biochemistry* **1997**, *36*, 7520−7526.
(5) Campbell, K. A.; Peloquin, J. M.; Pham, D. P.; Debus, R. J.; Britt, R. D. *J. Am. Chem. Soc.* **1998**, *120*, 447−448.
(6) Messinger, J.; Robblee, J. H.; Bergmann, U.; Fernandez, C.; Glatzel, P.; Visser, H.; Cinco, R. M.; McFarlane, K. L.; Bellacchio, E.; Pizarro, S. A.; Cramer, S. P.; Sauer, K.; Klein, M. P.; Yachandra, V. K. *J. Am. Chem. Soc.* **2001**, *123*, 7804−7820.
(7) Dau, H.; Iuzzolino, L.; Dittmer, J. *Biochim. Biophys. Acta* **2001**, *1503*, 24−39.
(8) Hoganson, C. W.; Babcock, G. T. *Science* **1997**, *277*, 1953−1956.
(9) Pecoraro, V. L.; Hsieh, W.-Y. In *Metal Ions in Biological Sytems*; Sigel, A., Sigel, H., Eds.; Marcel Dekker: New York, 2000; Vol. 37, pp 429−504.
(10) Vrettos, J. S.; Brudvig, G. W. *Philos. Trans. R. Soc. London, Ser. B* **2002**, *357*, 1395−1404.
(11) Limburg, J.; Vrettos, J. S.; Liable-Sands, L. M.; Rheingold, A. L.; Crabtree, R. H.; Brudvig, G. W. *Science* **1999**, *283*, 1524−1527.
(12) Srinivasan, K.; Michaud, P.; Kochi, J. K. *J. Am. Chem. Soc.* **1986**, *108*, 2309−2320.
(13) Zhang, W.; Loebach, J. L.; Wilson, S. R.; Jacobsen, E. N. *J. Am. Chem. Soc.* **1990**, *112*, 2801−2803.
(14) Irie, R.; Noda, K.; Ito, Y.; Katsuki, T. *Tetrahedron Lett.* **1991**, *32*, 1055−1058.
(15) Collins, T. J.; Gordon-Wylie, S. W. *J. Am. Chem. Soc.* **1989**, *111*, 4511−4513.
(16) Collins, T. J.; Powell, R. D.; Slebodnick, C.; Uffelman, E. S. *J. Am. Chem. Soc.* **1990**, *112*, 899−901.
(17) MacDonnell, F. M.; Fackler, N. L. P.; Stern, C.; O'Halloran, T. V. *J. Am. Chem. Soc.* **1994**, *116*, 7431−7432.
(18) Templeton, D. K.; Templeton, L. K. *Acta Crystallogr., Sect. A* **1980**, *A36*, 237−241.
(19) Penner-Hahn, J. E.; Benfatto, M.; Hedman, B.; Takahashi, T.; Doniach, S.; Groves, J. T.; Hodgson, K. O. *Inorg. Chem.* **1986**, *25*, 2255−2259.
(20) Lim, M. H.; Rohde, J. U.; Stubna, A.; Bukowski, M. R.; Costas, M.; Ho, R. Y. N.; Munck, E.; Nam, W.; Que, L. *Proc. Natl. Acad. Sci. U.S.A.* **2003**, *100*, 3665−3670.
(21) Rohde, J. U.; In, J. H.; Lim, M. H.; Brennessel, W. W.; Bukowski, M. R.; Stubna, A.; Munck, E.; Nam, W.; Que, L. *Science* **2003**, *299*, 1037−1039.
(22) Nam, W.; Choi, S. K.; Lim, M. H.; Rohde, J. U.; Kim, I.; Kim, J.; Kim, C.; Que, L. *Angew. Chem., Int. Ed.* **2003**, *42*, 109−111.
(23) Wolter, T.; Meyer-Klaucke, W.; Muther, M.; Mandon, D.; Winkler, H.; Trautwein, A. X.; Weiss, R. *J. Inorg. Biochem.* **2000**, *78*, 117−122.
(24) Penner-Hahn, J. E.; Eble, K. S.; McMurry, T. J.; Renner, M.; Balch, A. L.; Groves, J. T.; Dawson, J. H.; Hodgson, K. O. *J. Am. Chem. Soc.* **1986**, *108*, 7819−7825.
(25) Procedures for sample preparation, data collection, and data analysis are given in Supporting Information.
(26) Riggs, P. J.; Mei, R.; Yocum, C. F.; Penner-Hahn, J. E. *J. Am. Chem. Soc.* **1992**, *114*, 10650−10651.

JA0494104